

**Seismic scattering and absorption properties of Mars
estimated through coda analysis on a long-period
surface wave of S1222a marsquake**

Keisuke Onodera¹, Takuto Maeda², Kiwamu Nishida¹, Taichi Kawamura³,

Sabrina Menina³, Ludovic Margerin⁴, Philippe Lognonné³, William Bruce Barnerdt⁵

¹Earthquake Research Institute, The University of Tokyo, Tokyo, Japan

²Hirosaki University, Aomori, Japan

³Institut de Physique du Globe de Paris, Université Paris Cité, CNRS, Paris, France

⁴Institut de Recherche en Astrophysique et Planétologie, Université Toulouse III, CNRS, CNES, Toulouse, France.

⁵Jet Propulsion Laboratory, California Institute of Technology, California, USA

Contents of this file

Figures S1 to S4

Introduction

This document includes the information, which is not included in the main text, to help readers better understand our study. In the following document, we present three supporting figures related to (1) the background noise level, (2) theoretical curves related to grid search in the main text, (3) constraining Q_s , and (4) the scaled energy factor. These topics are related to the description in Section 1 and 6 in the main text.

Supporting Figures S1 – S4

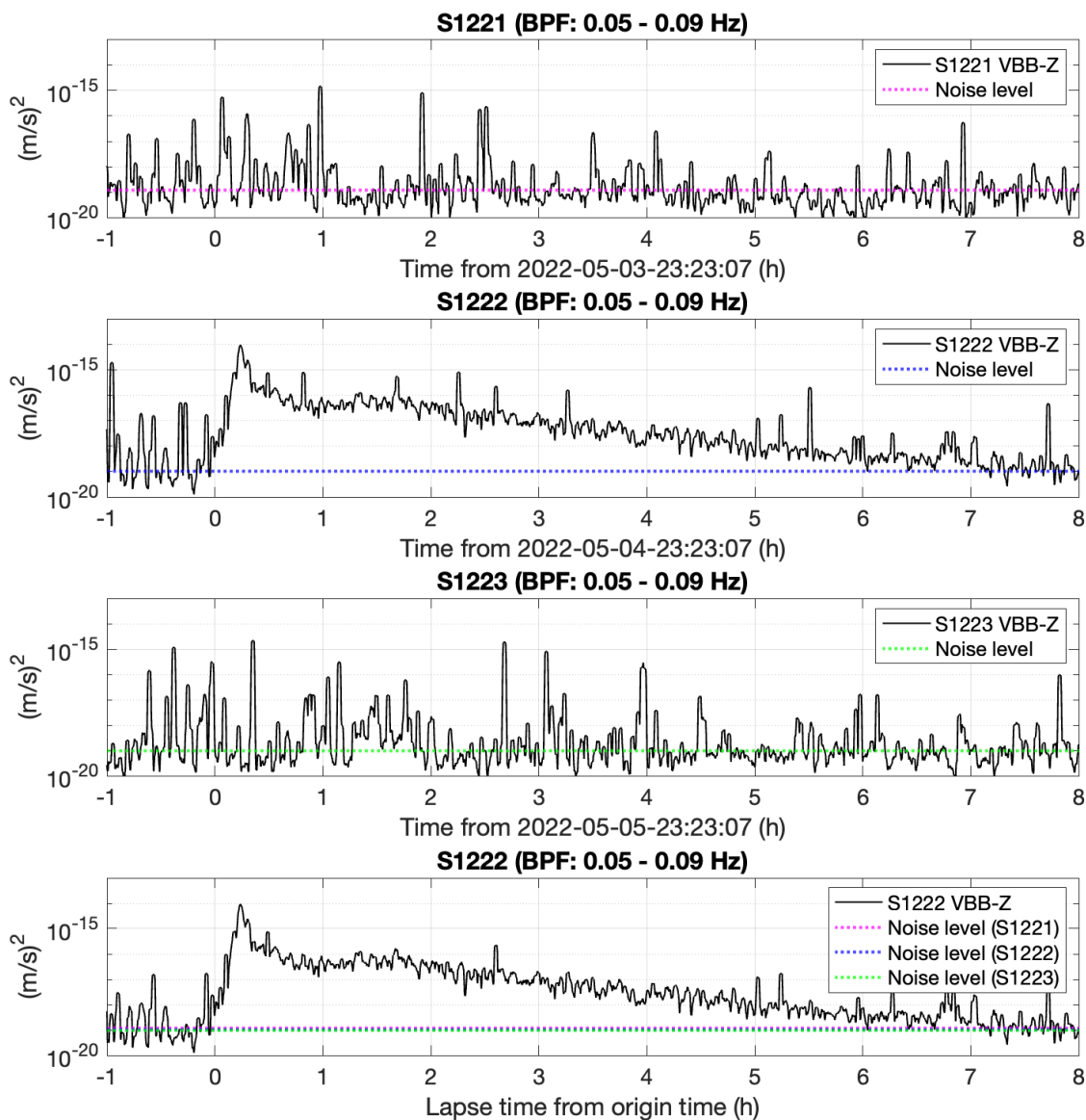


Figure S1. Comparison of noise level between Sol1221, Sol1222, and Sol1223. The top three figures show the vertical mean squared (MS) envelopes (black) and the noise levels (colored) at each sol. For Sol1221 and S1223, the noise level was estimated with the median value for the nine hour time window. Regarding Sol1222, the noise level was estimated using the time window before the origin time (< 0 h). The bottom figure compares the noise levels on Sol1221, Sol1222, and Sol1223. The black profile is the deglitched MS envelope on S1222 including S1222a marsquake.

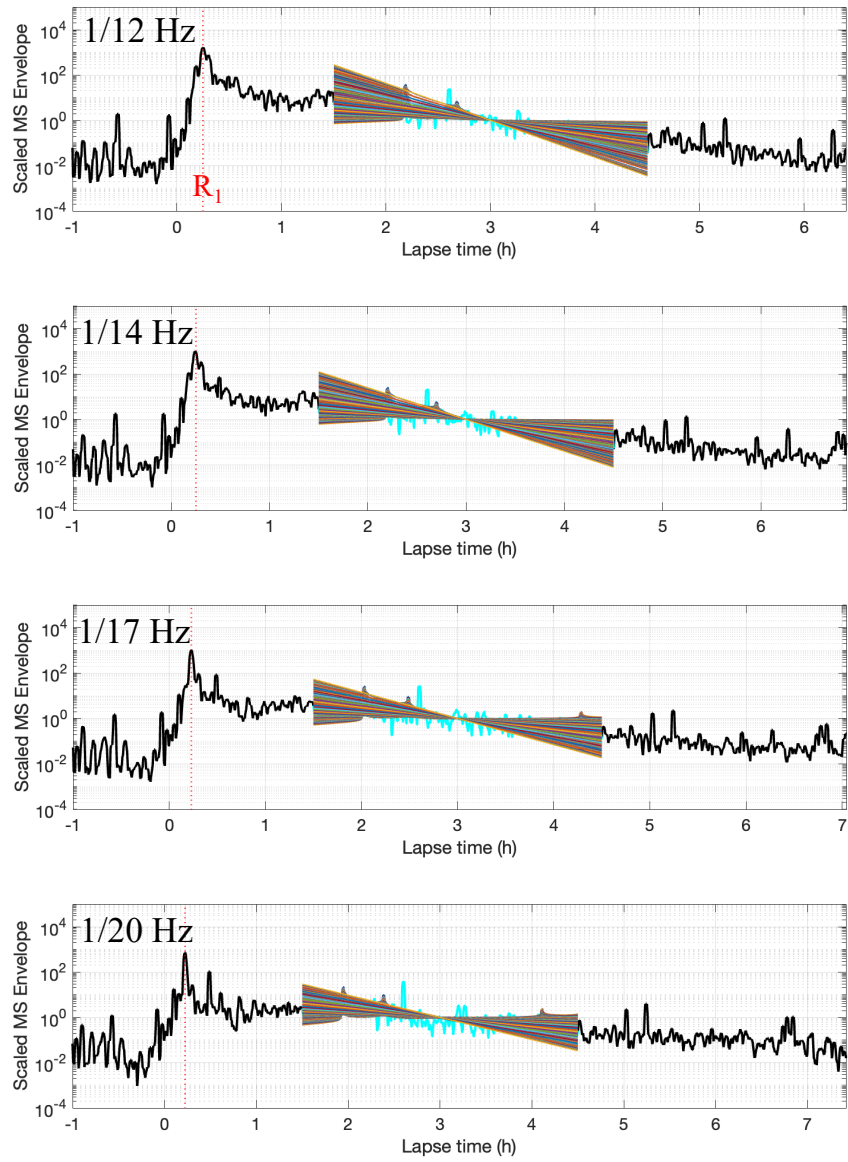


Figure S2. Representation of all of the calculated theoretical curves (colored) superposed on the observed MS envelope (black and cyan). For the fitting, the MS envelope for the time window of 1.5 – 3.5 h was used. The amplitude is scaled with the average amplitude between 1.5 – 3.5 h time window. The red dotted line shows the R_1 arrival.

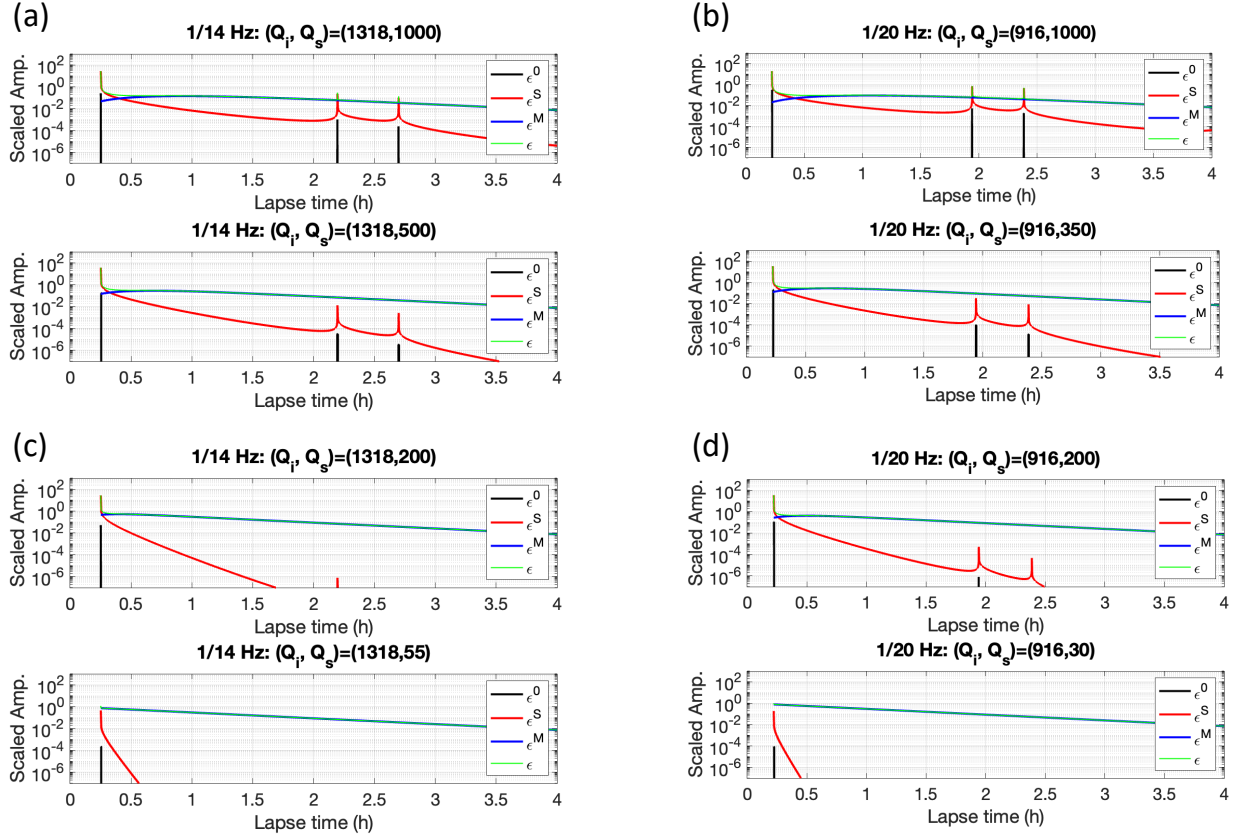


Figure S3. (a)-(b) Examples of parameter study results to estimate the upper limit of Q_s at 1/14 Hz and 1/20 Hz. The black lines are the direct wave component, the red profile is the single-scattered component, the blue is the multiple-scattered component, and the green is the convolved profile. The first row is for $Q_s = 1000$, where the multi-orbital phases are clearly seen (e.g., R_2 and R_3). The second row is the case for the upper limit of Q_s , where the contribution of the multiple scattering is strong enough to bury the multi-orbital phases. **(c)-(d)** Examples of parameter study results to estimate the lower limit of Q_s at 1/14 Hz and 1/20 Hz. The first row is for $Q_s = 200$, where the R_1 phase is clearly seen. The second row is the case for the lower limit of Q_s , where the contribution of the multiple scattering is strong enough to bury the R_1 phase.

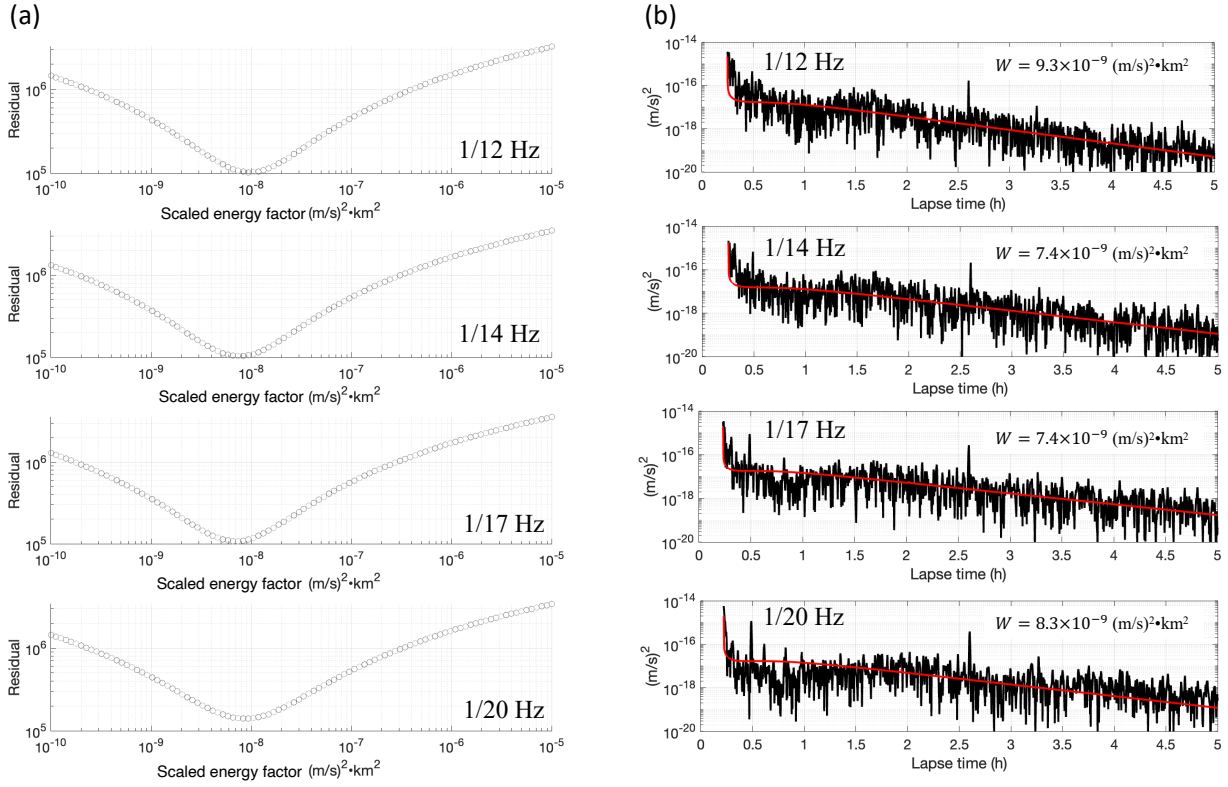


Figure S4. (a) Trace of the residual with the scaled energy factor. The summation of residual was calculated for each scaled energy factor in the same manner as Equation 8 in the main text. In that calculation, Q_i for each frequency band was fixed to the best-fitted value presented in Figure 3 in the main text, and Q_s was fixed to the upper limit that is described in Section 6 in the main text. **(b)** Comparison of the best-fitted curve (red) and the observed MS envelope (black). The most preferable scaled energy factor for the respective frequency bands is shown in the upper right corner in each panel.